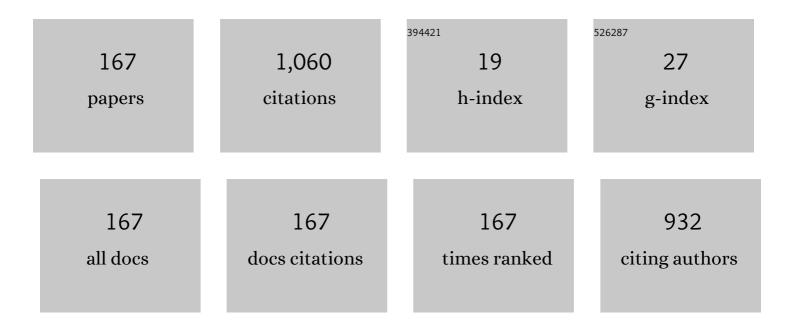
## List of Publications by Year in descending order

Source: https://exaly.com/author-pdf/4759790/publications.pdf Version: 2024-02-01



#	Article	IF	CITATIONS
1	Terahertz Emission Enhancement of Gallium-Arsenide-Based Photoconductive Antennas by Silicon Nanowire Coating. IEEE Transactions on Terahertz Science and Technology, 2022, 12, 36-41.	3.1	2
2	Indirect stress and air-cavity displacement measurement of MEMS tunable VCSELs via micro-Raman and micro-photoluminescence spectroscopy. Semiconductor Science and Technology, 2022, 37, 035013.	2.0	1
3	Integrated optics spiral photoconductive antennas coupled with 1D and 2D micron-size terahertz-wavelength plasmonic metal arrays. Optical Materials Express, 2022, 12, 1617.	3.0	4
4	Tunneling dynamics and transport in MBE-grown GaAs/AlGaAs asymmetric double quantum wells investigated via photoluminescence and terahertz time-domain spectroscopy. Journal of Materials Science: Materials in Electronics, 2022, 33, 16126-16135.	2.2	0
5	Terahertz emission increase in GaAs films exhibiting structural defects grown on Si (100) substrates using a two-layered LTG-GaAs buffer system. Journal of Materials Science: Materials in Electronics, 2021, 32, 13825-13836.	2.2	1
6	Effect of heteroepitaxial growth on LT-GaAs: ultrafast optical properties. Journal of Physics Condensed Matter, 2021, 33, 315704.	1.8	1
7	Spintronic terahertz emission from Ni/Pt bilayer grown on MgO. Journal of Physics: Conference Series, 2021, 1943, 012035.	0.4	0
8	Terahertz generation in a thin GaAs slab in a tapered parallel plate waveguide by femtosecond laser excitation at 1560Ânm. Japanese Journal of Applied Physics, 2021, 60, 072009.	1.5	1
9	Thickness dependence of the spintronic terahertz emission from Ni/Pt bilayer grown on MgO via electron beam deposition. Applied Physics Express, 2021, 14, 093001.	2.4	5
10	Creating terahertz pulses from titanium-doped lithium niobate-based strip waveguides with 1.55Âμm light. Journal of Materials Science: Materials in Electronics, 2021, 32, 23164-23173.	2.2	1
11	Interplay of Zn(OAc)2 concentration, morphology, and emission in hydrothermal-grown ZnO nanostructures. Journal of Crystal Growth, 2021, , 126339.	1.5	0
12	Ultrafast carrier dynamics and THz conductivity in epitaxial-grown LT-GaAs on silicon for development of THz photoconductive antenna detectors. Journal Physics D: Applied Physics, 2020, 53, 095105.	2.8	4
13	Terahertz transmission spectroscopy of soil minerals for geoarchaeological evaluation of sediments excavated from Pinagbayanan Batangas Philippines. Infrared Physics and Technology, 2020, 111, 103568.	2.9	2
14	Graphene transfer passivates GaAs. Applied Physics Letters, 2020, 117, .	3.3	4
15	A modulation-doped heterostructure-based terahertz photoconductive antenna emitter with recessed metal contacts. Scientific Reports, 2020, 10, 19926.	3.3	3
16	Observation of enhanced terahertz emission in two-dimensional metal line arrays on GaAs surfaces. Japanese Journal of Applied Physics, 2020, 59, 070907.	1.5	2
17	Spray Pyrolysis Deposition of Alâ€Đoped ZnO Thin Films for Potential Picosecond Extreme Ultraviolet Scintillator Applications. Physica Status Solidi (B): Basic Research, 2020, 257, 1900481.	1.5	2
18	Temperature-dependent terahertz time-domain spectroscopy of 3D, 2D, and 0D semiconductor heterostructures. Journal of Materials Science: Materials in Electronics, 2020, 31, 6321-6327.	2.2	1

#	Article	IF	CITATIONS
19	True bulk As-antisite defect in GaAs(1Â1Â0) identified by DFT calculations and probed by STM/STS measurements. Applied Surface Science, 2020, 511, 145590.	6.1	8
20	Low-temperature carrier dynamics in MBE-grown InAs/GaAs single- and multi-layered quantum dots investigated via photoluminescence and terahertz time-domain spectroscopy. Optical Materials Express, 2020, 10, 178.	3.0	6
21	Trilayer low-temperature-grown GaAs terahertz emitter and detector device with doped buffer. Applied Physics Express, 2020, 13, 082012.	2.4	3
22	Enhanced terahertz emission of silicon nanowire-coated gallium arsenide photoconductive antenna. , 2020, , .		0
23	Effect of substrate material on LT-GaAs carrier dynamics at 800 nm. , 2020, , .		0
24	Effect of Doped Buffer in Low-Temperature-Grown GaAs Terahertz Photoconductive Antenna Emitters and Detectors. , 2020, , .		0
25	Electro-Optic Sampling of Terahertz Pulses by using GaAs and Tapered Parallel Plate Waveguide. , 2020, , .		0
26	Enhanced terahertz emission of a gallium arsenide thin film on a porous silicon distributed Bragg reflector designed at 800nm wavelength. Optical Materials, 2019, 92, 335-340.	3.6	0
27	Photoconductivity, carrier lifetime and mobility evaluation of GaAs films on Si (100) using optical pump terahertz probe measurements. Semiconductor Science and Technology, 2019, 34, 035031.	2.0	13
28	Efficacy of proposed 2DEG-based photoconductive antenna using magnetic bias-controlled carrier transport. Current Applied Physics, 2019, 19, 756-761.	2.4	3
29	Atomically-resolved interface imaging and terahertz emission measurements of gallium arsenide epilayers. Journal of Applied Physics, 2019, 126, .	2.5	6
30	High Sensitivity Heterodyne Electro-Optic Sampling with 1.5-Â $\mu$ m Laser Source. , 2019, , .		0
31	Metal-Coated <100>-Cut GaAs Coupled to Tapered Parallel-Plate Waveguide for Cherenkov-Phase-Matched Terahertz Detection: Influence of Crystal Thickness. Journal of Infrared, Millimeter, and Terahertz Waves, 2018, 39, 514-520.	2.2	2
32	Epitaxial growth of p-InAs on GaSb with intense terahertz emission under 1.55-μm femtosecond laser excitation. Thin Solid Films, 2018, 648, 46-49.	1.8	1
33	Temperature dependence of THz emission and junction electric field of GaAs–AlGaAs modulation-doped heterostructures with different i-AlGaAs spacer layer thicknesses. Journal of Materials Science: Materials in Electronics, 2018, 29, 8760-8766.	2.2	4
34	Sensitivity Improvement of Heterodyne Electro-Optic Sampling. , 2018, , .		0
35	Photo-carrier dynamics of MBE-grown GaAs on Silicon studied by optical-pump terahertz-probe. , 2018, , .		2

E S ESTACIO

#	Article	IF	CITATIONS
37	Terahertz Emission Enhancement of i-/n-Gallium Arsenide Thin Film on a Porous Silicon Distributed Bragg Reflector designed at 800nm. , 2018, , .		0
38	Photoluminescence and terahertz time-domain spectroscopy of MBE-grown single-layered InAs/GaAs quantum dots. , 2018, , .		0
39	Surface effect of n-GaAs cap on the THz emission in LT-GaAs. Journal of Materials Science: Materials in Electronics, 2018, 29, 12436-12442.	2.2	1
40	Intense THz emission in high quality MBE-grown GaAs film with a thin n-doped buffer. Optical Materials Express, 2018, 8, 1463.	3.0	3
41	Terahertz emission characteristics of GaMnAs dilute magnetic semiconductor under 650ÂmT external magnetic field. Current Applied Physics, 2017, 17, 522-526.	2.4	2
42	Terahertz emission and photoluminescence of silicon nanowires electrolessly etched on the surface of silicon (100), (110), and (111) substrates for photovoltaic cell applications. Photonics and Nanostructures - Fundamentals and Applications, 2017, 24, 1-6.	2.0	7
43	Luminescence and carrier dynamics in nanostructured silicon. Journal of Luminescence, 2017, 186, 312-317.	3.1	2
44	Tunneling at room temperature in GaAs/AlGaAs asymmetric coupled double quantum wells observed via time resolved photoluminescence spectroscopy. Superlattices and Microstructures, 2017, 109, 324-329.	3.1	2
45	Structural and optical characterization and scintillator application of hydrothermal-grown ZnO microrods. Optical Materials, 2017, 65, 82-87.	3.6	11
46	Charge carrier dynamics of GaAs/AlGaAs asymmetric double quantum wells at room temperature studied by optical pump terahertz probe spectroscopy. Japanese Journal of Applied Physics, 2017, 56, 111203.	1.5	4
47	Defect-related temperature dependence of THz emission from GaAs/AlGaAs MQWs grown on off- and on-axis substrates. AlP Advances, 2017, 7, 125210.	1.3	3
48	Terahertz Emission from CuO Nanowires Synthesized Through Thermal Oxidation of Cu Foils. Science of Advanced Materials, 2017, 9, 193-198.	0.7	2
49	Enhanced Terahertz Emission and Raman Signal from Silicon Nanopyramids. Science of Advanced Materials, 2017, 9, 214-219.	0.7	1
50	Terahertz emission enhancement in semi-insulating gallium arsenide integrated with subwavelength one-dimensional metal line array. Optics Letters, 2016, 41, 4515.	3.3	5
51	Cherenkov-phase-matched nonlinear optical detection and generation of terahertz radiation via GaAs with metal-coating. Optics Express, 2016, 24, 24980.	3.4	8
52	Low temperature-grown GaAs carrier lifetime evaluation by double optical pump terahertz time-domain emission spectroscopy. Optics Express, 2016, 24, 26175.	3.4	16
53	Cherenkov-type generation and detection of terahertz radiation in a GaAs with metal-coat structure. , 2016, , .		0
54	Development of Resistance-Based pH Sensor Using Zinc Oxide Nanorods. Journal of Nanoscience and Nanotechnology, 2016, 16, 6102-6106.	0.9	12

#	Article	IF	CITATIONS
55	Porosity dependence of terahertz emission of porous silicon investigated using reflection geometry terahertz time-domain spectroscopy. Superlattices and Microstructures, 2016, 100, 892-899.	3.1	4
56	Al-doped ZnO and N-doped CuxO thermoelectric thin films for self-powering integrated devices. Materials Science in Semiconductor Processing, 2016, 45, 27-31.	4.0	24
57	Electro-optic sampling of terahertz pulses using BaTiO <inf>3</inf> in non-collinear Cherenkov phase-matching scheme. , 2015, , .		0
58	Temperature behavior of unstrained (GaAs/AlGaAs) and strained (InGaAs/GaAs) quantum well bandgaps. Optical and Quantum Electronics, 2015, 47, 3053-3063.	3.3	3
59	Enhanced terahertz emission from SI-GaAs with a sub-wavelength 1D metal array. , 2015, , .		0
60	Increased terahertz emission from SI-GaAs deposited with sub-wavelength spacing metal line array. , 2015, , .		0
61	Cu <sub>2</sub> ZnSnSe <sub>4</sub> photovoltaic thin film: A potential large-area THz emitter. , 2015, ,		0
62	Interruption-assisted epitaxy of faceted p-InAs on buffered GaSb for terahertz emitters. Applied Physics Express, 2015, 8, 035501.	2.4	3
63	Non-collinear electro-optic sampling techniques for efficient detection of THz radiation. , 2015, , .		0
64	Confined photocarrier transport in InAs pyramidal quantum dots via terahertz time-domain spectroscopy. Optics Express, 2015, 23, 14532.	3.4	9
65	Dynamics of Optically-Generated Carriers in Si (100) and Si (111) Substrate-Grown GaAs/AlGaAs Core-Shell Nanowires. Nanoscale Research Letters, 2015, 10, 1050.	5.7	2
66	Blue-shifted and picosecond amplified UV emission from aqueous chemical grown ZnO microrods. Optical Materials, 2015, 48, 179-184.	3.6	4
67	Noncollinear Electro-Optic Sampling of Terahertz Waves in a Thick GaAs Crystal. IEEE Transactions on Terahertz Science and Technology, 2015, 5, 732-736.	3.1	13
68	Terahertz emission from aluminum-doped ZnO–nGaAs heterostructure investigated using reflection-mode terahertz time-domain spectroscopy. Applied Physics Express, 2015, 8, 122101.	2.4	1
69	Tin Oxide-Silver Composite Nanomaterial Coating for UV Protection and Its Bactericidal Effect on Escherichia coli (E. coli). Coatings, 2014, 4, 320-328.	2.6	7
70	Terahertz surface emission from Cu2ZnSnSe4 thin film photovoltaic material excited by femtosecond laser pulses. Applied Physics Letters, 2014, 105, .	3.3	6
71	Frequency-resolved detection of broadband THz waves with Cherenkov-phase-matched heterodyne EO sampling. , 2014, , .		1
72	Terahertz emission enhancement in low-temperature-grown GaAs with an n-GaAs buffer in reflection and transmission excitation geometries. Journal of the Optical Society of America B: Optical Physics, 2014, 31, 291.	2.1	18

#	Article	IF	CITATIONS
73	Highly sensitive electro-optic sampling of terahertz waves using field enhancement in a tapered waveguide structure. Applied Physics Express, 2014, 7, 112401.	2.4	16
74	Shell to core carrier-transfer in MBE-grown GaAs/AlGaAs core–shell nanowires on Si(100) substrates. Journal of Luminescence, 2014, 155, 27-31.	3.1	3
75	Enhanced terahertz emission from GaAs substrates deposited with aluminum nitride films caused by high interface electric fields. Applied Surface Science, 2014, 303, 241-244.	6.1	3
76	Mapping of temporal coherence function for ultrafast lasers via statistical fringe analysis of reconstructed phase maps. Optics Communications, 2014, 329, 190-195.	2.1	7
77	Coherence Length Measurement for Ultra-short Laser Pulses Using Digital Holography and Statistical Fringe Analysis. , 2014, , 247-250.		0
78	Saturation and Polarization Characteristics of 1.56Âμm Optical Probe Pulses in a LTG-GaAs Photoconductive Antenna Terahertz Detector. Journal of Infrared, Millimeter, and Terahertz Waves, 2013, 34, 423-430.	2.2	8
79	Terahertz emission from GaAs-AlGaAs core-shell nanowires on Si (100) substrate: Effects of applied magnetic field and excitation wavelength. Applied Physics Letters, 2013, 102, .	3.3	20
80	Deep level traps and the temperature behavior of the photoluminescence in GaAs/AlGaAs multiple quantum wells grown on off-axis and on-axis substrates. Journal of Luminescence, 2013, 143, 517-520.	3.1	3
81	Photocarrier Transport and Carrier Recombination Efficiency in Vertically Aligned Si Nanowire Arrays Synthesized Via Metal-Assisted Chemical Etching. Applied Physics Express, 2013, 6, 082101.	2.4	5
82	Non-ellipsometric detection of terahertz radiation using heterodyne EO sampling in the Cherenkov velocity matching scheme. Optics Express, 2013, 21, 9277.	3.4	38
83	Lens Coupler and Magnetic Field Terahertz Emission Enhancement in InSb and InAs under 1.55-µm Excitation. Japanese Journal of Applied Physics, 2013, 52, 032201.	1.5	3
84	Detection of THz radiation by using GaAs in Cherenkov-phase-matched electro-optic sampling. , 2013, , .		1
85	Techniques of non-collinear electro-optic sampling for efficient detection of pulsed terahertz radiation. , 2013, , .		1
86	Influence of metal surface roughness on the phase velocity of terahertz waves propagating in parallel plate waveguides. , 2013, , .		2
87	Fast-Scan Terahertz Time Domain Spectrometer Based on Laser Repetition Frequency Modulation. Japanese Journal of Applied Physics, 2013, 52, 022401.	1.5	14
88	Terahertz emission from Indium Oxide films grown on MgO substrates using sub-bandgap photon energy excitation. Optics Express, 2012, 20, 4518.	3.4	1
89	Intense terahertz emission from molecular beam epitaxy-grown GaAs/GaSb(001). Journal of Applied Physics, 2012, 112, .	2.5	3
90	Enhancement of THz EO sampling efficiency using waveguides. , 2012, , .		0

E S ESTACIO

#	Article	IF	CITATIONS
91	Cherenkov phase-matched EO sampling of terahertz pulses using heterodyne scheme. , 2012, , .		0
92	Photoconductive Emission and Detection of Terahertz Pulsed Radiation Using Semiconductors and Semiconductor Devices. Journal of Infrared, Millimeter, and Terahertz Waves, 2012, 33, 393-404.	2.2	21
93	Efficient electro-optic sampling detection of terahertz radiation via Cherenkov phase matching. Optics Express, 2011, 19, 19901.	3.4	46
94	Efficient generation and electro-optic sampling detection of THz radiation using Cherenkov phase matching scheme. , 2011, , .		1
95	Terahertz Emission from GaAs Films on Si(100) and Si(111) Substrates Grown by Molecular Beam Epitaxy. Journal of Infrared, Millimeter, and Terahertz Waves, 2011, 32, 418-425.	2.2	2
96	Intense terahertz emission from undoped GaAs/n-type GaAs andÂInAs/AISb structures grown on Si substrates in the transmission-geometry excitation. Applied Physics B: Lasers and Optics, 2011, 103, 825-829.	2.2	8
97	Micro-pulling-down-method-grown Ce:LiCAF crystal for side-pumped laser amplifier. Journal of Crystal Growth, 2011, 318, 737-740.	1.5	7
98	Terahertz emission from indium oxide films on MgO substrates excited at a photon energy below the bandgap. , 2011, , .		0
99	Efficient electro-optic sampling detection and generation of intense THz radiation via Cherenkov-type phase matching in a LiNbO <inf>3</inf> crystal coupled to a Si prism. , 2011, , .		0
100	Intense terahertz emission from GaAs and InAs thin films grown on GaSb substrates. , 2011, , .		0
101	Enhancement of terahertz emission from InSb using a lens coupler and magnetic field. , 2011, , .		0
102	ZnO Scintillator Improved Temporal Response for XFEL Timing Observation. , 2010, , .		0
103	Custom-designed scintillator for laser fusion diagnostics – Pr3+-doped fluoro-phosphate lithium glass scintillator. Optical Materials, 2010, 32, 1393-1396.	3.6	11
104	Response-time improved hydrothermal-method-grown ZnO scintillator for XFEL timing-observation. Optical Materials, 2010, 32, 1305-1308.	3.6	13
105	Investigation of the terahertz emission characteristics of MBE-grown GaAs-based nanostructures. Optical Materials, 2010, 32, 776-779.	3.6	1
106	Note: Light output enhanced fast response and low afterglow L6i glass scintillator as potential down-scattered neutron diagnostics for inertial confinement fusion. Review of Scientific Instruments, 2010, 81, 106105.	1.3	14
107	Response-time improved hydrothermal-method-grown ZnO scintillator for soft x-ray free-electron laser timing-observation. Review of Scientific Instruments, 2010, 81, 033102.	1.3	25
108	Down-scattered neutron imaging detector for areal density measurement of inertial confinement fusion. Review of Scientific Instruments, 2010, 81, 10D303.	1.3	7

#	Article	lF	CITATIONS
109	Numerical Approach for Determination of Cutback Length to Estimate Dispersion and Loss Parameters of Terahertz Waveguides. Japanese Journal of Applied Physics, 2010, 49, 072702.	1.5	0
110	Observation of Complex Optical Processes in ZnSe under Extreme Optical Excitation from a Kilojoule-Class Nd:Glass Laser. Japanese Journal of Applied Physics, 2010, 49, 062601.	1.5	0
111	Er:LiCAF as Potential Vacuum Ultraviolet Laser Material at 163 nm. IEEE Transactions on Nuclear Science, 2010, 57, 1204-1207.	2.0	24
112	\${hbox {Nd}}^{3+}{hbox {:LaF}}_{3}\$ as a Step-Wise Excited Scintillator for Femtosecond Ultraviolet Pulses. IEEE Transactions on Nuclear Science, 2010, 57, 1208-1210.	2.0	25
113	Er:LiCAF as Potential Vacuum Ultraviolet Laser Material at 163 nm. , 2009, , .		0
114	Enhanced terahertz emission from GaAs in MBE-grown InAs/GaAs quantum dot structures. , 2009, , .		0
115	Amplification of Ultraviolet Femtosecond Pulse by a Micro-Pulling Down Method-Grown Ce:LiCAF Crystal in a Prismatic Cell-Type, Side-Pumping Configuration. Japanese Journal of Applied Physics, 2009, 48, 120213.	1.5	8
116	Development of Vacuum Ultraviolet Streak Camera System for the Evaluation of Vacuum Ultraviolet Emitting Materials. Japanese Journal of Applied Physics, 2009, 48, 096503.	1.5	21
117	Vacuum ultraviolet luminescence from a micro-pulling-down method grown Nd3+:(La0.9,Ba0.1)F2.9. Journal of Luminescence, 2009, 129, 1629-1631.	3.1	28
118	Observation of birefringence in BBO crystals in the terahertz regime. Journal of Crystal Growth, 2009, 311, 895-898.	1.5	3
119	Transmission characteristics of lens-duct and photonic crystal waveguides in the terahertz region. Journal of the Optical Society of America B: Optical Physics, 2009, 26, A95.	2.1	3
120	Strong enhancement of terahertz emission from GaAs in InAs/GaAs quantum dot structures. Applied Physics Letters, 2009, 94, 232104.	3.3	24
121	Pr3+-doped fluoro-oxide lithium glass as scintillator for nuclear fusion diagnostics. Review of Scientific Instruments, 2009, 80, 113504.	1.3	41
122	Three-photon Lasing from ZnSe Excited by a kilojoule-class Nd:Glass Laser. , 2009, , .		0
123	Transmission of terahertz radiation using a microstructured polymer optical fiber. Optics Letters, 2008, 33, 902.	3.3	109
124	Vacuum ultraviolet optical properties of a micro-pulling-down-method grown Nd^3+:(La_09,Ba_01)F_29. Journal of the Optical Society of America B: Optical Physics, 2008, 25, B27.	2.1	18
125	Laser Quality Ce <sup>3+</sup> :LiCaAlF <sub>6</sub> Grown by Micro-Pulling-Down Method. Japanese Journal of Applied Physics, 2008, 47, 5605.	1.5	22
126	Transverse magnetic field polarity effects on the terahertz radiation from GaAs/AlGaAs modulation-doped heterostructures with varying AlGaAs spacer-layer thickness. Journal of Applied Physics, 2008, 104, 073506.	2.5	5

#	Article	IF	CITATIONS
127	Birefringence of β-BaB2O4 crystal in the terahertz region for parametric device design. Applied Physics Letters, 2008, 92, .	3.3	19
128	Interband dot-to-well transitions in InAsâ^•InGaAs dots in a well probed via photocurrent and electroluminescence spectroscopy. Applied Physics Letters, 2008, 92, .	3.3	2
129	Experimental and calculated terahertz spectra of naphthalene and 1,4-dihydroxynaphthalene in the 0.5 - 6 terahertz region. Journal of Physics: Conference Series, 2008, 112, 042073.	0.4	2
130	Terahertz birefringence of β-BaB2O4 (BBO) crystal. , 2008, , .		0
131	Optical Properties of Micro-Pulling Down Method Grown Nd3+:(La1-x,Bax)F3-x as Potential Vacuum Ultraviolet Laser Material and Scintillator. The Review of Laser Engineering, 2008, 36, 1303-1305.	0.0	0
132	Micro-pulling down method grown Ce:LiCAF as ultraviolet laser. , 2008, , .		0
133	Nd <sup>3+</sup> :(La <sub>1-x</sub> ,Bax)F <sub>3-x</sub> as vacuum ultraviolet scintillator and new laser material. , 2007, , .		Ο
134	Nd <sup>3+</sup> :(La <sub>1-x</sub> Ba <sub>x</sub> )F <sub>3-x</sub> Grown by Micro-Pulling Down Method as Vacuum Ultraviolet Scintillator and Potential Laser Material. Japanese Journal of Applied Physics, 2007, 46, L985.	1.5	23
135	Magnetic-field-induced fourfold azimuthal angle dependence in the terahertz radiation power of (100) InAs. Applied Physics Letters, 2007, 90, 151915.	3.3	22
136	Azimuthal symmetry folding in the terahertz radiation power of (100) p-InAs under 1 Tesla magnetic field. , 2007, , .		0
137	Nd <sup>3+</sup> : (La <inf>1-x</inf> ,Ba <inf>x</inf> )F <inf>3-x</inf> as Vacuum Ultraviolet Scintillator and New Laser Material. , 2007, , .		0
138	Numerical calculations of the Frequency Spectra of naphthalene and 1,4-dihydroxynaphthalene in the 0.5-to 6 terahertz region. , 2007, , .		0
139	Planar terahertz waveguide using CYTOP; a highly transparent plastic feasible for hybrid optics applications. , 2007, , .		0
140	Nd3+: (La1-x, Bax)F3-x Grown via Micro-PD as New Vacuum Ultraviolet Scintillator and Potential Laser Material. , 2007, , .		0
141	Proposed design principle of fluoride-based materials for deep ultraviolet light emitting devices. Optical Materials, 2007, 30, 15-17.	3.6	45
142	Improvement of the Photoluminescence Decay Response Characteristics of an Oxide-confined Vertical Cavity Surface Emitting Laser Probed by Femtosecond Laser Pulses. Springer Series in Optical Sciences, 2007, , 325-331.	0.7	0
143	Action Spectra of GaAs/AlGaAs Multiple Quantum Wells Exhibiting Terahertz Emission Peak at Excitation Energies Below the Bandgap. Springer Series in Optical Sciences, 2007, , 307-315.	0.7	0
144	Terahertz (THz) Pigtail Assembly Utilizing a Lens Duct for Effective Coupling of THz Radiation into Teflon Photonic Crystal Fiber Waveguide. Springer Series in Optical Sciences, 2007, , 293-299.	0.7	0

#	Article	IF	CITATIONS
145	Terahertz Radiation from Photoconductive Switch Fabricated from a Zinc Oxide Single Crystal. Springer Series in Optical Sciences, 2007, , 301-306.	0.7	0
146	Observation of Four-fold Azimuthal Angle Dependence in the Terahertz Radiation Power of (100) p-InAs. , 2006, , .		0
147	Below-bandgap excited, terahertz emission of optically pumped GaAs/AlGaAs multiple quantum wells. Journal of Photochemistry and Photobiology A: Chemistry, 2006, 183, 334-337.	3.9	3
148	Low-loss single-mode terahertz waveguiding using Cytop. Applied Physics Letters, 2006, 89, 211119.	3.3	26
149	Terahertz - time domain spectroscopy of microstructured poly(methylmetacrylate) polymer fiber. , 2006, , .		0
150	Magnetic field orientation dependence of the terahertz radiation from GaAs/AlGaAs modulation-doped structures with varying AlGaAs spacer-layer thickness. , 2006, , .		0
151	Photoluminescence decay characteristics of an oxide-confined vertical-cavity surface-emitting laser. Applied Physics Letters, 2006, 88, 121122.	3.3	0
152	Terahertz radiation from (100) p-InAs under 1 tesla magnetic field due to surge current. , 2006, , .		0
153	Low-loss single-mode THz waveguiding using CYTOP, a highly transparent plastic with potential as hybrid optics. , 2006, , .		0
154	Terahertz transmission spectroscopic analysis of mono- and di-substituted hydroxynaphthalenes in the 0.5- to 6- THz region using GaP THz wave generator. , 2006, , .		0
155	Terahertz radiation in below-bandgap, optically pumped GaAs/AlGaAs multiple quantum wells in magnetic field. , 2005, , .		0
156	Photonic-crystal-fiber pigtail device integrated with lens-duct optics for terahertz radiation coupling. Applied Physics Letters, 2005, 87, 151114.	3.3	18
157	Raman spectroscopy ofin situannealed InAs/GaAs quantum dots. Journal of Applied Physics, 2004, 96, 1267-1269.	2.5	4
158	Time response characteristics of an oxide-confined GaAsâ^•AlGaAs resonant cavity-enhanced photodetector. Applied Physics Letters, 2004, 85, 3011-3013.	3.3	1
159	Observation of blue-shifted photoluminescence in stacked InAs/GaAs quantum dots. Journal of Crystal Growth, 2003, 251, 196-200.	1.5	11
160	Observation of high junction electric fields in modulation-doped GaAs/AlGaAs heterostructures by room temperature photoreflectance spectroscopy. Journal of Applied Physics, 2002, 91, 3717-3720.	2.5	11
161	Observation of blue shifted photoluminescence in stacked InAs/GaAs quantum dots. , 0, , .		0
162	Uncharacteristic behaviour in low temperature of conductive polypyrrole detected by temperature-dependent terahertz transmission spectroscopy. , 0, , .		0

E S ESTACIO

#	Article	IF	CITATIONS
163	Modal analysis of Teflon photonic crystal fiber as a terahertz waveguide. , 0, , .		Ο
164	Zinc oxide single crystal as substrate for photoconductive antenna device generating radiation in the terahertz frequency region. , 0, , .		1
165	Observation of below-bandgap excited terahertz emission in the action spectra of GaAs/AlGaAs multiple quantum wells. , 0, , .		О
166	Channeling terahertz (THz) radiation into a Teflon photonic crystal fiber waveguide by means of a lens duct in a THz pigtail assembly. , 0, , .		0
167	Atomically Precise Delineation of As Antisite Defect States from Undoped Gallium Arsenide Host Lattice by Scanning Tunneling Microscopy and Spectroscopy Measurements and Density Functional Theory Calculations. Physica Status Solidi (B): Basic Research, 0, , 2100652.	1.5	1